



Observation of Boundary Layer Transition on a Sharp Cone with a Porous Surface

Jungmu Hur. Jinhwi Kim. Junhyuk Nam. Jinyoung Kim. Bok Jik Lee⁵

Abstract

Laminar-turbulent transition in hypersonic boundary layers causes a large increase in surface heat flux and imposes severe aerothermal loads on vehicles. Passive attenuation of boundary-layer disturbances relevant to laminar-turbulent transition using porous surfaces was investigated on a half-smooth, halfporous sharp cone tested in the Seoul National University Hypersonic Shock Tunnel at Mach 6.76. Two configurations were evaluated, a uniform porous surface tuned to the Mack second-mode band measured on the smooth side, and a non-uniform porous surface that mixed two hole diameters to absorb lower frequencies not attenuated by the uniform surface. Surface-pressure and heat-flux measurements were combined with schlieren visualization to document instability growth and breakdown. On the smooth side, Mack second-mode waves amplified and broke down to turbulence. Both porous surfaces reduced the Mack second-mode peak in the pressure spectra, and the non-uniform porous surface provided greater attenuation. Consistently, the time-averaged surface heat flux on the porous side was reduced by approximately 40% relative to the smooth side. The results indicate that appropriately designed porous surfaces can attenuate Mack second-mode disturbances and reduce associated heating on sharp cones.

Keywords: hypersonic, boundary layer transition, Mack second-mode instability, surface heat flux reduction

Nomenclature

 h_{total} - Freestream total enthalpy [MJ/kg] x – Streamwise coordinate along cone slant [mm] M – Mach number Re_{unit} – Unit Reynolds number [10⁶/m]

1. Introduction

In hypersonic flight, laminar-turbulent transition in the boundary layer increases surface heat flux and imposes severe aerothermal loads on vehicles. This rise in surface heating can necessitate more robust thermal protection system (TPS) designs, increasing the mass of the TPS. Understanding and controlling the transition process is therefore essential for reliable hypersonic vehicle design.

In sharp-nosed hypersonic boundary layers, the Mack second mode is widely reported as a dominant route to transition. Using linear stability theory, Mack identified the second mode as a trapped acoustic

¹Department of Aerospace Engineering, Seoul National University, Seoul 08826, Republic of Korea, gjwjdan135@snu.ac.kr

²Department of Aerospace Engineering, Seoul National University, Seoul 08826, Republic of Korea, harrykim0814@snu.ac.kr

³Department of Aerospace Engineering, Seoul National University, Seoul 08826, Republic of Korea, njh970101@snu.ac.kr

⁴Department of Aerospace Engineering, Seoul National University, Seoul 08826, Republic of Korea, kimted@snu.ac.kr

⁵Department of Aerospace Engineering, Seoul National University, Seoul 08826, Republic of Korea, b.lee@snu.ac.kr

pressure wave that amplifies by reflections between the wall and the boundary layer edge. Its dominant frequency varies with Mach number and Reynolds number, and thus with streamwise position [1].

Following Mack's work, porous coatings designed to provide acoustic absorption in the second-mode frequency band have been explored as a means to mitigate laminar—turbulent transition. Fedorov et al. predicted stabilization by porous coatings using linear stability theory [2]. Rasheed et al. demonstrated attenuation of second-mode waves and delay of transition in hypersonic wind-tunnel experiments using an ultrasonically absorptive surface [3]. These results show that appropriately designed porous surfaces reduce the Mack second-mode amplitude and delay transition.

Experiments were conducted with a sharp cone model to assess the effectiveness of porous surfaces in attenuating the Mack second-mode instability. The model was half-smooth and half-porous, enabling direct comparison under identical freestream conditions. Two porous configurations were used: a uniform porous surface tuned to the Mack second-mode frequency measured on the smooth side, and a non-uniform porous surface that mixes two hole diameters to also absorb lower-frequency content. High-frequency pressure transducers and coaxial type E thermocouples measured surface-pressure disturbances and surface heat flux.

2. Experimental setup

2.1. Facility overview

All experiments were conducted in the Seoul National University Hypersonic Shock Tunnel (SHyST), as shown in Fig. 1. A contoured Mach 6.76 nozzle with an exit diameter of 341 mm was used, and the test section had windows of 500 mm width and 300 mm height. Table 1 lists the test flow conditions and schlieren coverage for each run. Six runs were performed under identical freestream conditions. The driver gas was 98% He and 2% N_2 by mole fraction. The nozzle reservoir pressure was steady for 2 ms with a standard deviation of 2%; a 1 ms core window within this period was used for analysis to avoid initial non-uniform nozzle flow and diaphragm debris effects. Characteristics of SHyST and its nozzle are documented by Kim et al. [4].

ID	Surface	Schlieren range [mm]	M	Re_{unit} [10 $^6/m$]	h_{total} [MJ/kg]
S1	Smooth	200-350	6.76	6.96	1.59
S2	Smooth	300-450	6.76	6.88	1.55
U1	Uniform porous	200-350	6.76	6.90	1.58
U2	Uniform porous	300-450	6.76	6.83	1.63
N1	Non-uniform porous	200-350	6.76	6.97	1.58
N2	Non-uniform porous	300–450	6.76	7.07	1.56

Table 1. Test flow conditions.

2.2. Test model and data acquisition

The test model was a sharp cone with a half-angle of 7° and a total length of 600 mm, in a half-smooth and half-porous configuration, as shown in Fig. 2(a). The conical frustum from x=150 to x=455 mm along the slant was covered by a thin, removable surface layer. One half was smooth and the other half was porous.

Two porous surface configurations were tested. The uniform porous surface had a hexagonal hole arrangement. The non-uniform porous surface mixed two hole diameters in a square arrangement to also absorb lower-frequency content. The dimensions and layouts of the porous surfaces are shown in Fig. 2 and listed in Table 2.

Eight PCB132 pressure transducers and sixteen Medtherm coaxial type E thermocouples were mounted along the cone surface, equally distributed between the smooth and porous sides. The sensor locations are shown in Fig. 3. Signals from the pressure transducers were acquired at 2.5 MHz and low-pass

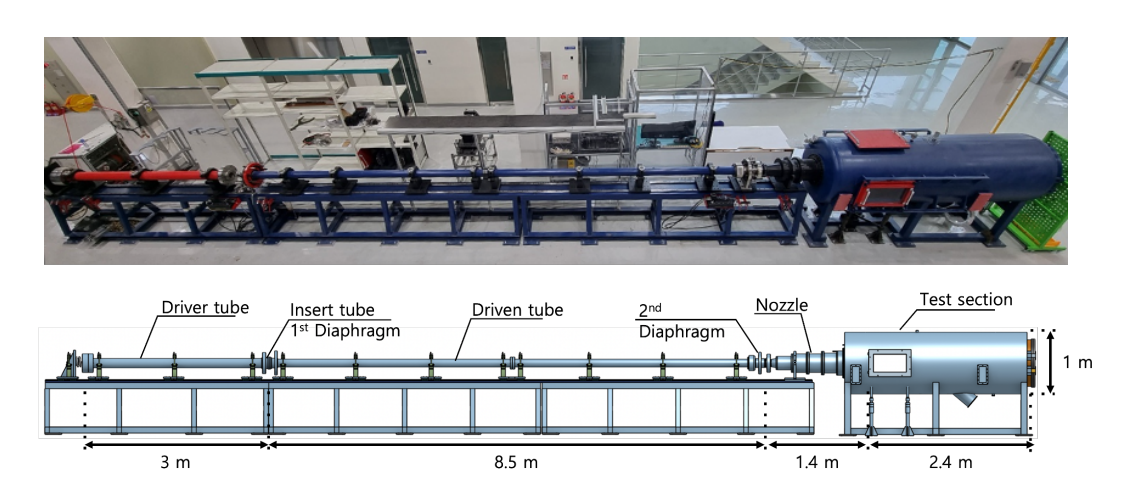


Fig 1. Overall view of the SHyST facility (top) and CAD model of the test section (bottom).

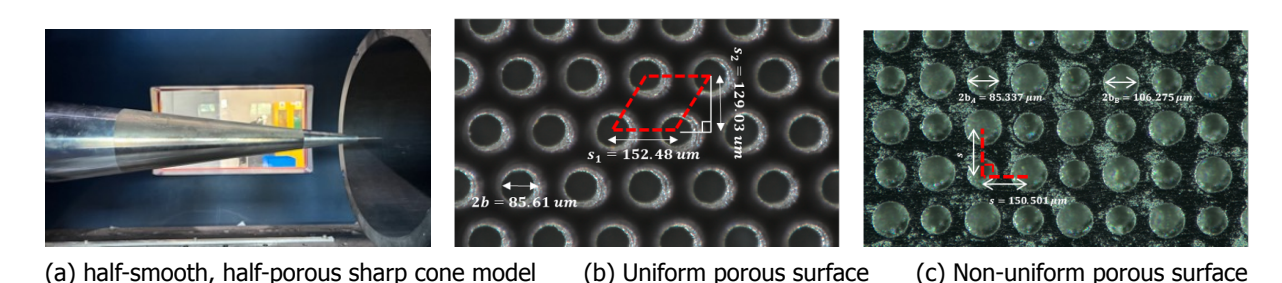


Fig 2. Photographs of the cone model and porous surfaces.

filtered at 1 MHz. Thermocouple signals were amplified by a factor of 500 and smoothed with a moving average filter with a 300-sample window.

Schlieren imaging covered the cone surface from x=150 to x=450 mm along the slant. Images of size 1280 \times 32 pixels were acquired at 1.5 MHz using a Phantom TMX 6410 high-speed camera. The horizontal field of view was 150 mm, and the exposure time was 0.095 μ s. Fig. 4 shows the Z-type schlieren setup used in this study.

3. Results

3.1. Schlieren visualization

As shown in Fig. 5, the smooth surface showed the rope-like structure of Mack second-mode waves near $x=250\,$ mm, followed by intermittent breakdown around $x=300\,$ mm. On the uniform porous surface, the rope-like pattern was absent; isolated transition events occurred at different streamwise positions. On the non-uniform porous surface, no breakdown was observed within the schlieren field of view.

3.2. Surface pressure disturbance

As shown in Fig. 6 (a–c), time histories of surface-pressure perturbations p' at x=227.5-437.5 mm are presented for (a) smooth, (b) uniform porous, and (c) non-uniform porous surfaces. Closer inspection of Fig. 6 (a) shows convecting wave packets characteristic of Mack second-mode activity that broaden in bandwidth downstream and intermittently reach large amplitudes, with the amplitude of p' consistently larger than on the porous cases. The uniform porous surface (b) lowers overall fluctuation levels relative to the smooth case but still exhibits a few intermittent large-amplitude packets. The non-uniform porous surface (c) maintains low amplitudes throughout the record, and comparable intermittent high-amplitude events are not observed.

Parameter	Uniform	Non-uniform (A)	Non-uniform (B)
Hole diameter	86	85	106
Hole depth	300	90	150
Unit-cell size $(x \times y)$	t-cell size $(x \times y)$ 152 × 129 150		× 150
Porosity (%)	29	3	2

Table 2. Dimensions of porous surface (manufactured values only). All lengths in μ m.

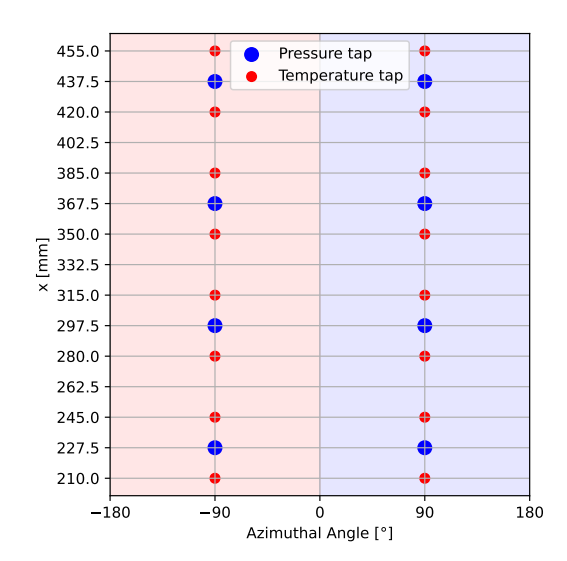


Fig 3. Sensor location map on the cone model.

Fig. 7(a) shows the power spectral density (PSD) of surface-pressure signals at $x=227.5\,$ mm; all cases exhibit a pronounced peak near 700 kHz consistent with the Mack second-mode instability, and a second peak around 300 kHz that likely corresponds to a harmonic of the Mack second-mode instability content or to a structural/acoustic resonance of the cone. Fig. 7(b) shows the PSD at $x=297.5\,$ mm; both porous surfaces substantially attenuate the 700 kHz peak, whereas the smooth surface displays broadband energy indicative of breakdown to turbulence near this station. The peak near 300 kHz remains little affected for the smooth and uniform porous surfaces but is strongly reduced for the non-uniform porous surface, plausibly due to larger-diameter perforations that target lower frequencies. Fig. 7(c) shows the PSD at $x=367.5\,$ mm; the smooth surface exhibits elevated levels over a wide band (200–800 kHz), the uniform porous surface effectively damps the 700 kHz band but has relatively higher levels near 400 kHz, and the non-uniform porous surface continues to suppress both the 300 kHz and 700 kHz bands. Fig. 7(d) shows the PSD at $x=437.5\,$ mm; the smooth and porous surfaces present broadband, high-amplitude spectra indicative of post-transition turbulence, whereas the non-uniform porous surface maintains comparatively low amplitudes across the band.

3.3. Surface heat flux

Fig. 8a shows the streamwise distribution of the time-averaged surface heat flux for each surface. On the smooth side, the heat flux begins to rise from x=245 mm, consistent with the rope-like Mack second-mode structure observed in schlieren at x=200-250 mm. A pronounced jump appears near x=315 mm, in line with transition occurring around x=300 mm. Downstream of this station, the heat flux decreases toward x=420 mm as the post-transition boundary layer thickens along the cone.

On the porous sides, the heat flux remains below that of the smooth surface over most of the measured range. The uniform and non-uniform configurations show similar shapes upstream; however, the uniform porous surface exhibits a local increase near $x=400\,$ mm, which is consistent with a rare within-run

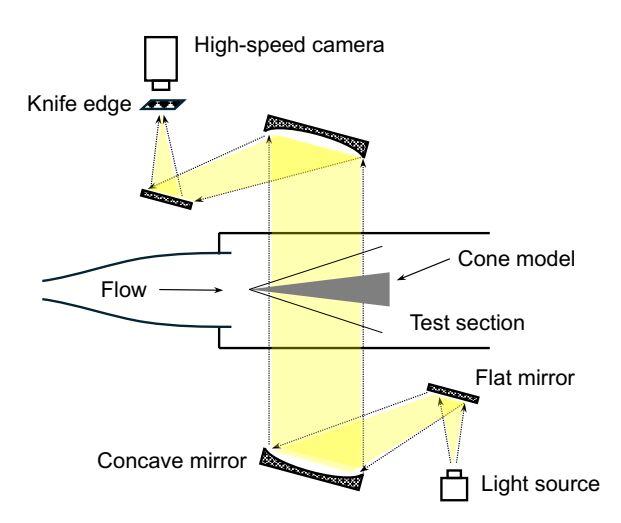


Fig 4. Schematic of the schlieren setup.

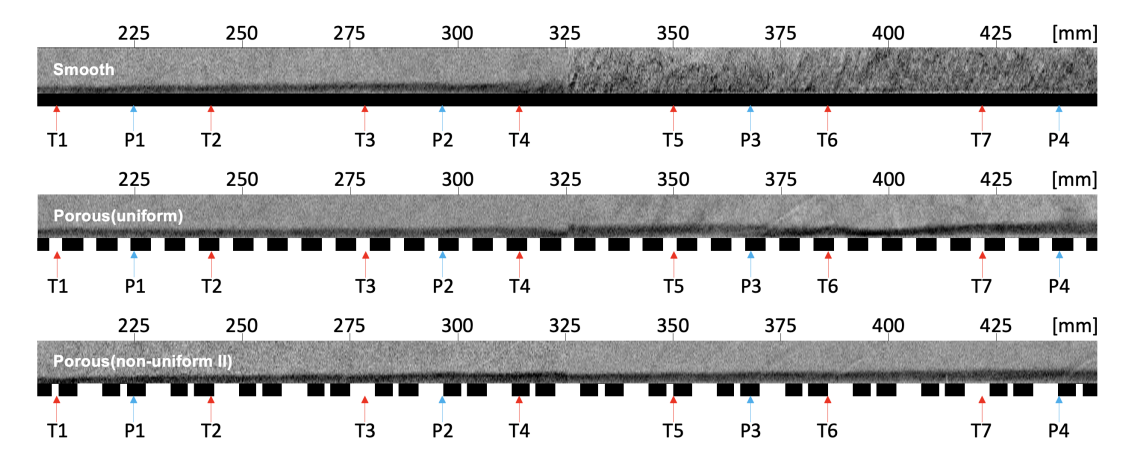


Fig 5. Schlieren visualization of the cone surface: from top to bottom, smooth surface, uniform porous surface, and non-uniform porous surface.

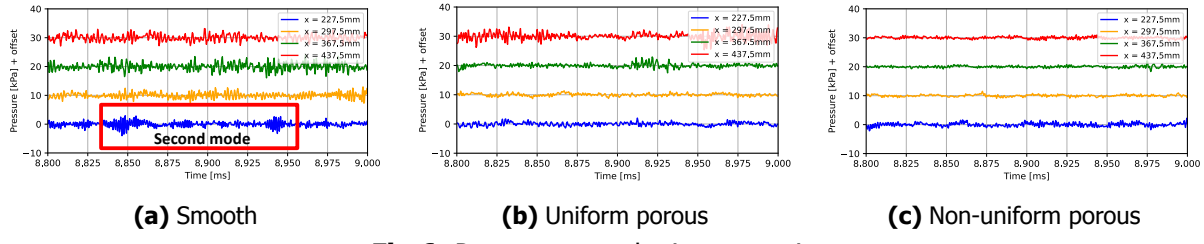


Fig 6. Pressure perturbations over time

transition event during the useful test time. In contrast, the non-uniform porous surface maintains comparatively low levels through the aft stations.

Fig. 8b presents the heat flux ratio of the porous surfaces relative to the smooth surface. Between x=245 and 385 mm, the porous configurations reduce the heat flux by approximately 40%.

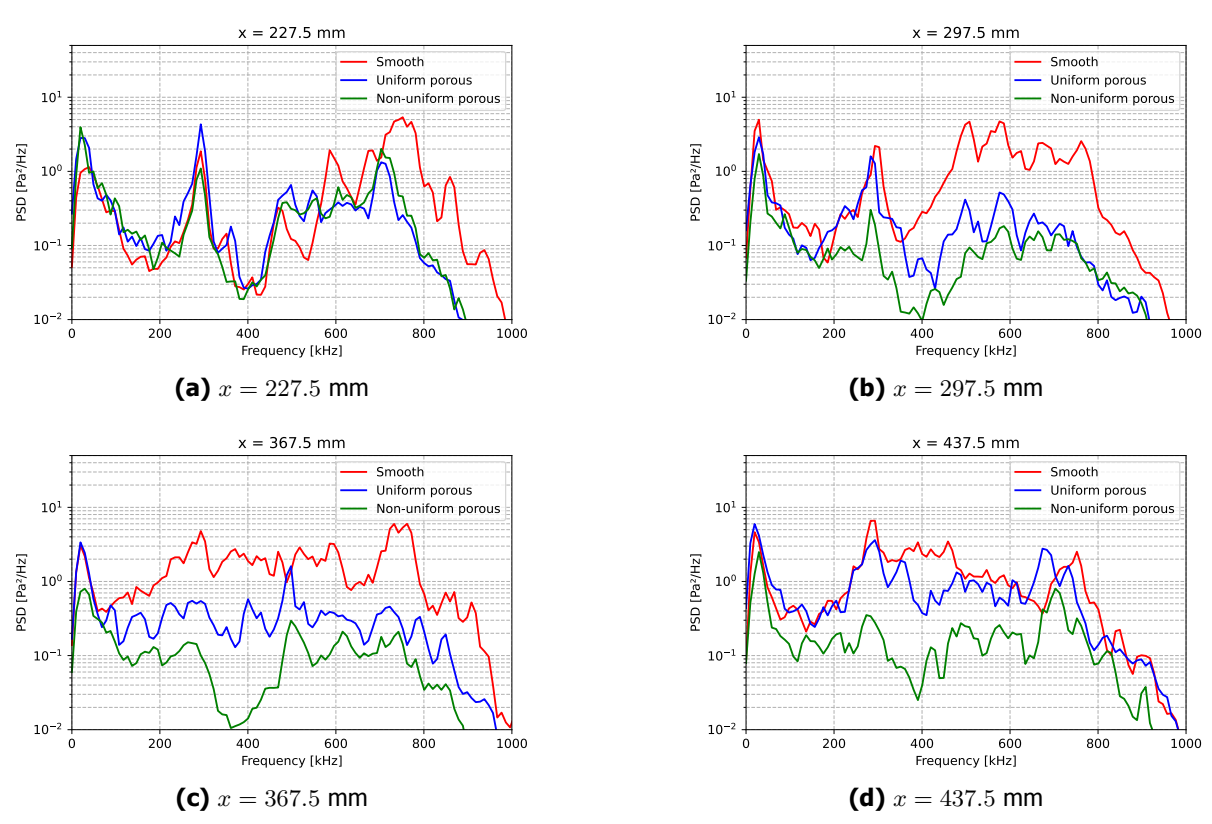
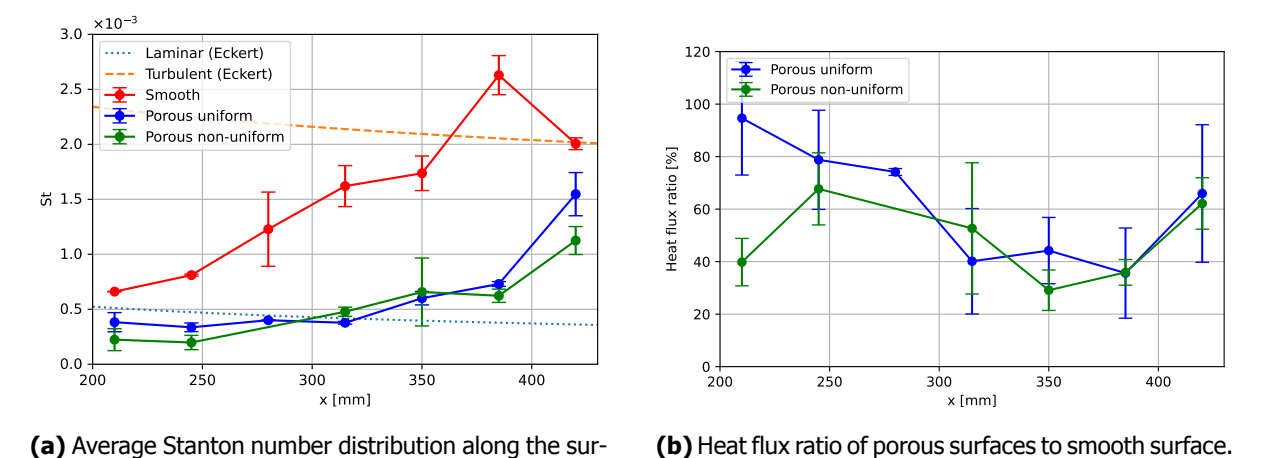


Fig 7. Power spectral density comparisons at different measurement positions for Smooth, uniform, and non-uniform porous surfaces.



face.

Fig 8. Comparison of measured surface heat flux between smooth and porous configurations.

4. Conclusions

Experiments in the SHyST facility on a half-smooth, half-porous sharp cone at Mach 6.76 were used to assess passive attenuation of Mack second-mode disturbances by porous surfaces. The main findings are as follows.

- 1. Flow visualization. Schlieren images showed rope-like Mack second-mode signatures on the smooth side near $x=250\,$ mm and intermittent breakdown around $x=300\,$ mm. The uniform porous surface removed the rope-like pattern but exhibited sporadic transition at wandering streamwise locations, whereas the non-uniform porous surface showed no visible breakdown within the present field of view.
- 2. **Pressure spectra.** Time histories and PSDs at $x=227.5,\ 297.5,\ 367.5,\ and\ 437.5$ mm confirmed that both porous configurations attenuate the 700 kHz Mack second-mode peak relative to the smooth surface. The non-uniform surface additionally suppresses energy near 300 kHz and maintains the lowest overall amplitudes across stations.
- 3. **Surface heat flux.** Relative to the smooth surface, the porous surface reduce time-averaged heat flux by approximately 40% between x=245 and 385 mm. A local increase on the uniform surface near x=400 mm is consistent with a rare within-run transition event.

Results demonstrate that porous surfaces can effectively attenuate disturbances and reduce aerothermal loading.

References

- [1] Leslie M Mack. Boundary-layer linear stability theory. Agard rep, 709, 1984.
- [2] Alexander V. Fedorov, Norman D. Malmuth, Adam Rasheed, and Hans G. Hornung. Stabilization of hypersonic boundary layers by porous coatings. *AIAA J.*, 39(4):605–610, 2001.
- [3] A. Rasheed, H. G. Hornung, A. V. Fedorov, and N. D. Malmuth. Experiments on passive hypervelocity boundary-layer control using an ultrasonically absorptive surface. *AIAA J.*, 40(3):481–489, 2002.
- [4] Jinyoung Kim, Jinhwi Kim, Jungmu Hur, Bok Jik Lee, and In-Seuck Jeung. Nozzle flow characterization of the SNU hypersonic shock tunnel. *Int. J. Aeronaut. Space Sci.*, 26(3):953–962, 2025.